Experimental Investigation of Spray Characteristics of Pre-Filming Air-Blast Atomizers II – Influence of Liquid Properties

M. Roudini[1†] and G. Wozniak[1, 2]

[1] Institute of Mechanics and Thermodynamics, Chemnitz University of Technology, Chemnitz, Germany
[2] Suvis GmbH, Chemnitz, Germany

†*Corresponding author email: mehrzad.roudini@s2013.tu-chemnitz.de*

ABSTRACT

One of the most important advantages of twin-fluid atomizers over other atomizers is the opportunity of atomizing liquids in a wide range of liquid properties efficiently. Thus, the fundamentals of spray dynamics, such as spray pattern, liquid breakup length, and spatial droplet size evolution using different liquid properties need to be investigated in some detail. The purpose of this study is therefore to examine and describe the influence of the liquid viscosity and surface tension on the spray performance of prefilming air-blast atomizers. A high-speed background shadowgraphy technique associated with particle tracking and Phase Doppler Anemometry (PDA) as a non-intrusive high-resolution local measurement technique were utilized to study the atomization process regarding the influence of the liquid properties on the spray quality. Generally, the break up mechanism is considerably influenced by the liquid viscosity. The breakup length (L_b) is dependent on liquid viscosity with $L_b \propto \mu_l^{0.30}$ and $L_b \propto \mu_l^{0.46}$ for P_a = 0.25 and 0.6 bar air pressure, respectively. Droplet size distribution profiles of different liquids in axial and radial directions are studied. No significant influences of the surface tension and viscosity were observed on the mean droplet velocity downstream of the spray. A minor increase of the droplet mean diameter was observed with liquid viscosity variations from 22 to 111 mPas, however, the liquid surface tension was verified to play an important role in the atomization process at prefilming airblast atomizers as well. According to the available experimental data, it has subsequently been possible to develop an original and descriptive model based on a dimensional approach at different air pressure ranges.

NOMENCLATURE

A	area	x	coordinate in radial direction
C	empirical constant		
d	characteristic length	μ	dynamic viscosity
d_e	outer diameter of tube	ν	kinematic viscosity
d_i	inner diameter of tube	ρ	density
D	gas slit diameter	σ	surface tension
GSMD	Global Sauter Mean Diameter		
L	length		
N	Nozzle number	Subscripts	
n	normal condition	a	air
P	pressure	b	breakup
Re	Reynolds number	e	outer
SMD	Sauter Mean Diameter	g	gas
U	velocity	I	inner
$Q, \dot{V}$	volume flow rate	l	liquid
We	Weber number	p	prefilming
z	coordinate in axial direction	rel	relative

1. INTRODUCTION

Generating small droplets from a bulk of liquids having a wide range of liquid properties is widespread in many technical processes and practical applications. However, most of the existing atomizers are not appropriate to atomize liquids with certain physical properties efficiently. One of the atomizers which is able to disintegrate effectively the liquids with a wide range of physical properties, particularly the viscosity, is an air blast atomizer. In air blast atomizers the liquid has usually a low velocity. Moreover, the initial aerodynamic air force will be opposed to the stabilizing viscous forces during the atomization process. In consequence, the resulting droplet sizes are less profound to liquid viscosity variations.

Particular physical properties of the liquid, such as viscosity, surface tension, and density affect the jet breakup mechanism (Lefebvre, 1989). The influence of the density will not be covered in the current study due to firstly a very small difference in the amount of density between most liquids and secondly a relatively small effect of the liquid density on the mean drop size in airblast atomizers (Lorenzetto & Lefebvre, 1977; Rizkalla & Lefebvre, 1975). Surface tension defines as a force that confronts the droplet surface formation. Furthermore, both the drop size distribution and the pattern of a spray beside the liquid flow in the nozzle are notably affected by variation of the liquid viscosity. According to earlier investigations, the viscosity is the most important liquid property since it influences distinctly the generated droplet size distribution depending on the atomizer internal flow and spray pattern (Lefebvre & McDonell, 2017). During droplet generation using any kind of atomizer, surface tension is an important parameter due to its competence to hinder new surface area formation (Lefebvre & McDonell, 2017). Therefore, viscosity and surface tension are important parameters in the atomization process. Lorenzetto investigated the influence of both physical properties on the Sauter mean diameter at a certain location in coaxial jet sprays (Lorenzetto & Lefebvre, 1977). It was observed that any increase in viscosity always increases the mean drop size. Moreover, surface tension forces also affect atomization adversely by opposing any distortion of the liquid surface.

In the previous literature, it has been shown that the resulting spray from airblast atomizers consists of two important regions. Firstly, the liquid film interaction with high turbulent air flow during primary atomization at the near field of the atomizer. Secondly, the spray development during the secondary atomization process at the far field region. The primary phase has been often unnoticed and is still a topic of ongoing research (Chaussonnet et al., 2018; Gepperth et al., 2013; Gepperth et al., 2012). The secondary breakup of droplets is generally understood (Guildenbecher et al., 2009; Hardalupas & Whitelaw, 1994; Urbán et al., 2017), however, the understanding of the effect of liquid properties on atomization mechanisms close to the atomizer exit and the detailed characteristics of the spray productivity are essentially required for the development and design of prefilming air-blast atomizers for specific applications.

Droplet size and droplet velocity in the spray developing region are the most important aspects to characterize spray production. Since a precise numerical calculation of the droplet size distribution after many random liquid breakup events was unattainable until now, a parametric analysis should be a good estimation method to attain empirical correlations between the mean drop sizes and operating conditions. The droplet size distribution was mainly modeled empirically and analytically by the existing literature (Babinsky & Sojka, 2002; Lefebvre, 1989; Liu et al., 2006; Sellens & Brzustowski, 1985; Urbán et al., 2017; Zhou & Yu, 2000). In a well-known correlation for the droplet diameter in an air-blast atomization, Rizk presented an empirical, dimensionally correct Eq. (1) which consists of two separate terms, one of which is dominated by the relative velocity and surface tension and the other by the viscosity (Rizk & Lefebvre, 1984):

$$\frac{SMD}{d_i} = 0.48 \left(\frac{\sigma}{\rho_g U_{rel}^2 d_i} \right)^{0.4} \left(1 + \frac{1}{ALR} \right)^{0.4}$$
$$+ 0.15 \left(\frac{\mu_l^2}{\sigma \rho_l d_i} \right)^{0.5} \left(1 + \frac{1}{ALR} \right) \tag{1}$$

where d_i, denotes the inner diameter of the liquid feeding tube, ρ_g the gas density, U_{rel} the velocity between air and the liquid jets at the exit, ALR the air to liquid mass flow rate ratio, μ the dynamic viscosity, σ the surface tension and the Sauter Mean diameter (SMD) as the diameter of the drop whose ratio of volume to surface area is the same for the entire spray. The SMD is a crucial parameter for mass transfer and combustion related applications of sprays (Lefebvre & McDonell, 2017). Equation 1 and the other investigated correlations are generally capable to explain the tendency of the SMD. However, they are rather valid for specific measurement positions and special cases.

In the current study, the influence of the liquid viscosity and surface tension on the breakup mechanism using different nozzle geometries are initially investigated. Then, the behavior of dispersed droplet dynamics, and droplet size spatial developments are examined locally using different liquid properties. In the first part, the liquid film breakup process near the nozzle exit will be carefully tracked using the shadowgraphy technique associated with particle tracking. Phase Doppler Anemometry (PDA) as the most sophisticated optical measurement technique used in spray analysis will be employed in the second part to investigate the spray performance. Finally, prediction approaches for the development and design of a prefilming air-blast atomizer will be quantified.
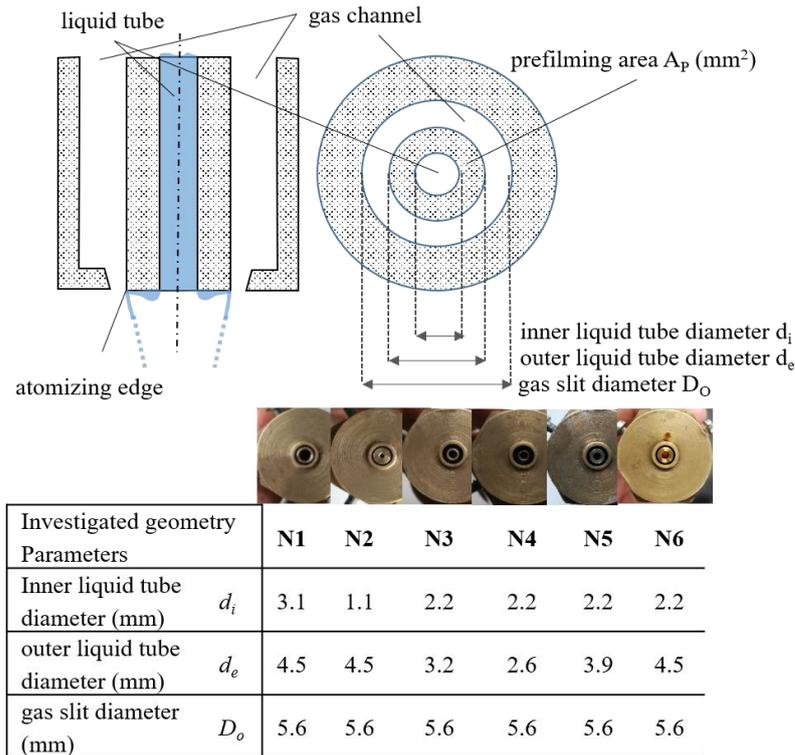
Investigated geometry Parameters		N1	N2	N3	N4	N5	N6
Inner liquid tube diameter (mm)	d_i	3.1	1.1	2.2	2.2	2.2	2.2
outer liquid tube diameter (mm)	d_e	4.5	4.5	3.2	2.6	3.9	4.5
gas slit diameter (mm)	D_o	5.6	5.6	5.6	5.6	5.6	5.6

Fig. 1. Investigated atomizer geometries.

2. EXPERIMENTAL SETUP AND MEASUREMENT TECHNIQUES

In the current study, a fundamentally important nozzle exit has been selected to avoid the complicated internal flow of most practical airblast atomizers. Important geometries and definitions on investigated nozzles are shown in Fig. 1.

A description of the air supply system, liquid supply, and experimental setup systems used in this study is provided by a previous publication from the same authors and will therefore not be repeated here (Roudini & Wozniak, 2018).

The liquid flowrate varies from 30 *ml/min* to 80 ml/min, corresponding to a Reynold number range from 5 to 83 in the liquid property's investigations. The air pressure varies from 0.25 bar to 0.6 bar, corresponding to a relative Weber number range from 56 to 317. Important non-dimensional numbers such as the relative Weber number and liquid Reynolds number are used in this study and shown in Eqs. (2) and (3).

$$We_{rel} = \frac{\rho_g (U_g - U_l)^2 d}{\sigma} \qquad (2)$$

$$Re_l = \frac{\rho_l U_l d}{\mu_l} \qquad (3)$$

ρ_l, ρ_g, σ, μ_l, U_l, U_g and d are liquid density, gas density, liquid surface tension, liquid viscosity, liquid velocity, gas velocity, characteristic length respectively.

Water and three different glycerol-water mixtures are employed in the current experiments to investigate the effect of liquid viscosity on liquid break up mechanisms close to the nozzle. The density, surface tension and viscosity at different shear rates of these fluids were measured prior to the atomization and results are given in Table 1.

Table 1 Physical and rheological properties of investigated liquids in flow visualization tests

Liquids	ρ	σ	μ	T
	[Kg/l]	[mN/m]	[mPas]	[K]
G 2 W 1	1.184	42.1 ± 0.10	22 ± 1.8	298
G 3 W 1	1.198	49.7 ± 0.29	38.4 ± 1.8	298
G 4 W 1	1.209	51.1 ± 0.23	61.6 ± 1.6	298
W	0.997	71.5	0.9	298

Furthermore, water, four different glycerol-water mixtures, and three different ethanol-water mixtures are employed in the experiments to investigate the effect of liquid viscosity and surface tension values on the droplet size and droplet velocity downstream the spray. The density, surface tension and viscosity of these fluids were measured prior to the atomization and results are given in Table 2.

Table 2 Physical and rheological properties of investigated liquids in PDA measurements

Liquids	ρ [Kg/l]	σ [mN/m]	μ [mPas]	T [K]
G 2 W 1	1.184	42.1 ± 0.10	22 ± 1.8	298
G 3 W 1	1.198	49.7 ± 0.29	38.4 ± 1.8	298
G 4 W 1	1.209	51.1 ± 0.23	61.6 ± 1.6	298
G 6 W 1	1.221	51.4 ± 0.21	111 ± 1.7	298
10 E 90 W	0.983	44.9 ± 0.05	1.2 ± 0.09	298
25 E 75 W	0.962	35.1 ± 0.05	1.9 ± 0.05	298
40 E 60 W	0.925	30 ± 0.05	1.8 ± 0.05	298
W	0.997	71.5	0.9	298

The viscosity of different liquids used in the atomization experiments was measured by a Rheometer (Physica UDS 200), manufactured by Anton Paar GmbH. The measuring drive is based on a highly dynamical motor-driven system with torque measurement and optical actuator. Surface tension and density were measured with a force Tensiometer named Attension Sigma 702 (Biolin Scientific AB) which offers high resolution and precision for surface and interfacial tension measurements by the Wilhelmy Plate method. All the measurements were taken under atmospheric pressure and at 298 K. The value of the surface tension was the average of at least five separate measurements. For the density measurement, a glass density probe with a known volume is hung from the balance hook and immersed into the liquid to be measured. The force needed to hold the probe at a constant depth in the liquid is then recorded. The software automatically calculates the density of the liquid using the principle of Archimedes. The liquid density was measured with a resolution of 0.0001 *g/cm³*.

A background shadowgraphy technique was implemented using a high-speed intensified camera to analyze the disintegration of the liquid near the nozzle exit. For spray analysis, PDA as a non-intrusive local measurement technique was applied which allows to measure the size, velocity and concentration of droplets in sprays. The measurement techniques and setups were explained in detail in the previous publication (Roudini & Wozniak, 2018). The measurement locations were set along the centerline from $x = 5$ mm to $x = 200$ mm with 40 equal distant measurement points to observe the spray quality at different axial distances from the nozzle. To observe radial droplet size distributions a plane with 21 measurement points was analyzed ($x = 100$ mm, $z = -15$ mm to 15 mm) (Fig. 2). Raw data from the PDA software (BSA Flow V.5.2) were exported and the statistical analysis and the data assessment were performed separately using appropriate software (OriginPro).
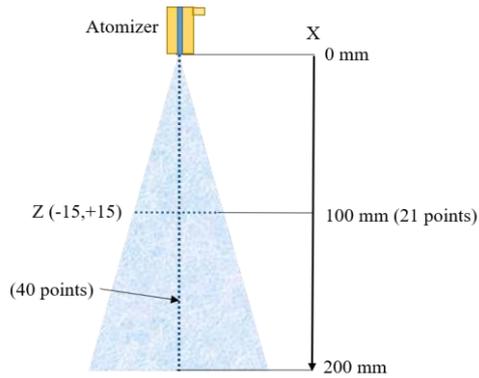
Fig. 2. PDA measurement locations.

3. EXPERIMENTAL RESULTS AND DISCUSSIONS

3.1. Flow Visualization

The liquid breakup mechanism and spray pattern close to the nozzle orifice were explored and explained in a wide range of the air pressure, water flowrate and nozzle geometry (Roudini & Wozniak, 2018). In this study, the influence of viscosity on the breakup mechanism in vicinity of the nozzle exit is investigated.

In Fig. 3, the effect of the liquid viscosity on the breakup mechanism during different operation conditions using nozzle 5 has been shown. Water and three different glycerol-water mixtures are employed. The viscosity generally was observed to delay the liquid disintegration by identical air and liquid flowrates. The liquid cone appeared to be larger and longer in higher viscosity operations. As the viscosity is increased at $P_a = 0.25$ bar (top to bottom in Fig. 3(a), membrane breakup events appear more likely and later very long ligaments were generated due to high viscosity internal forces. Indeed, generated droplets in the area of interest contain a wide size range including small and very big droplets. From the captured high-speed images, it can be observed that the changes in viscosity contribute to a lesser extend as the breakup mechanism in front of the atomizer in high air velocity compared to low air velocity conditions. In case of atomization of the Glycerol-Water mixture with the highest viscosity of 61.6 mPas, the surface stripping and small liquid subjet disintegration disappeared from the external surface of the liquid core due to a higher stabilization behavior of liquid viscosity (Fig. 3(b) and (c)). The main liquid disintegration occurred downstream of the spray where the liquid core jet breaks up. Increasing liquid flowrate from 50 ml/min to 80 ml/min with constant air conditions not only increases the breakup events in front of the atomizer similar to water but also increases the ligament and droplet size (Fig. 3(c) and (d)). The observations from this section agree well with previous conclusions of Lefebvre (Lefebvre, 1989). In very low air pressure measurements ($P_a = 0.25$ bar and $We_{rel} = 66$), the high viscous liquid stretches within a long distance from the nozzle orifice at N4 shown in Fig. 4. A liquid cone is generated followed by a thick liquid
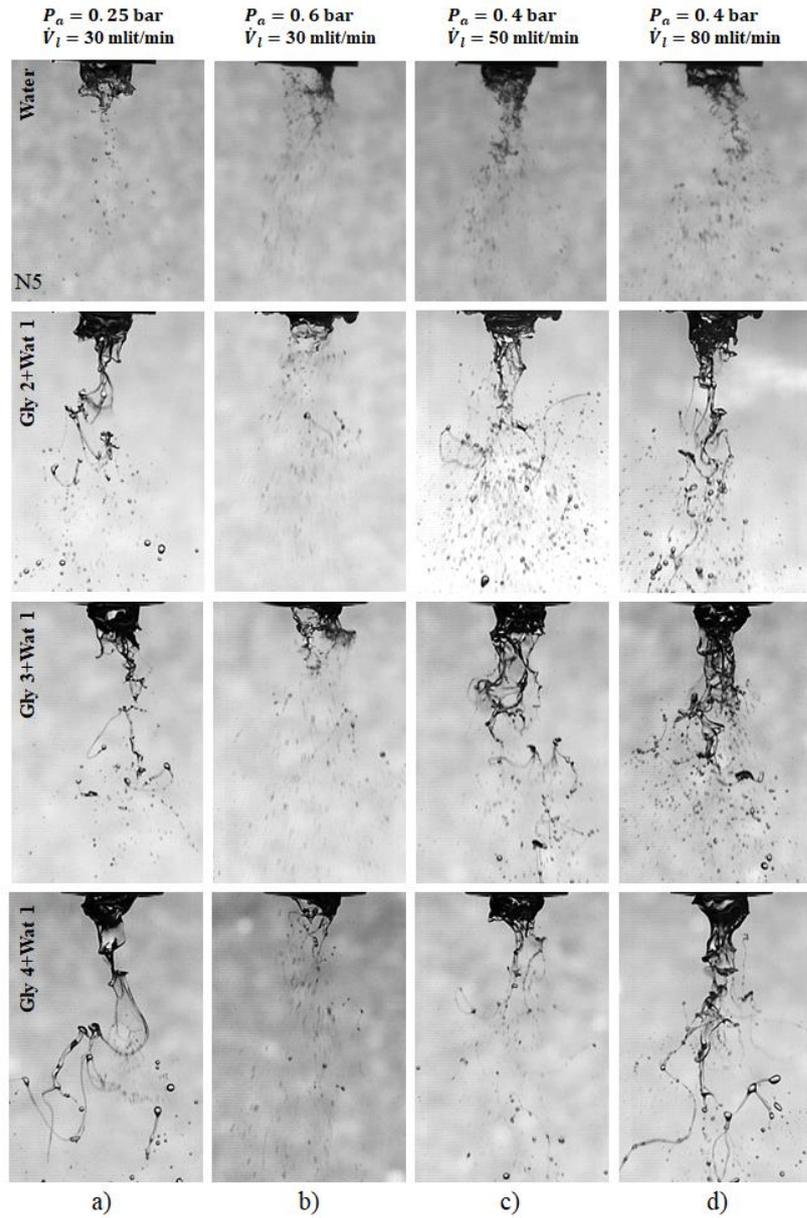
Fig. 3. Effect of the liquid viscosity on the liquid jet breakup mechanism at different operation conditions.
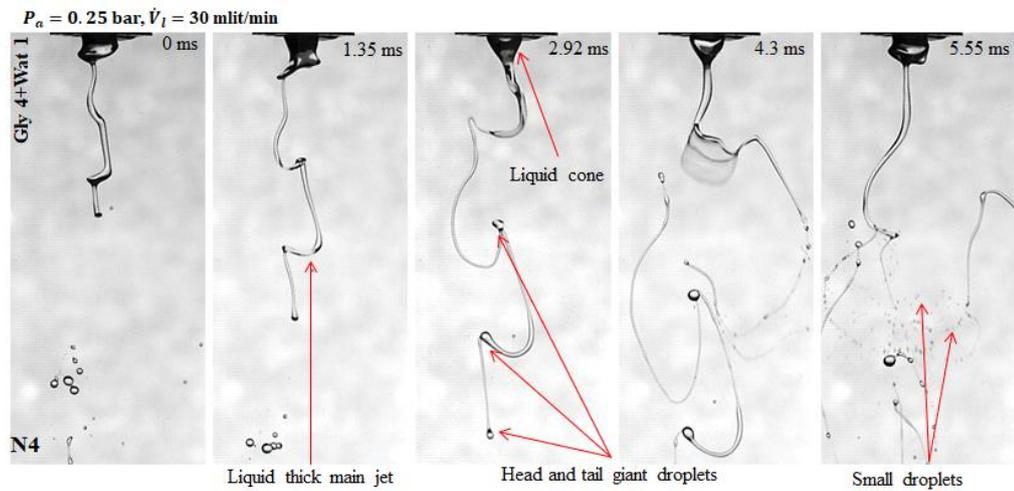

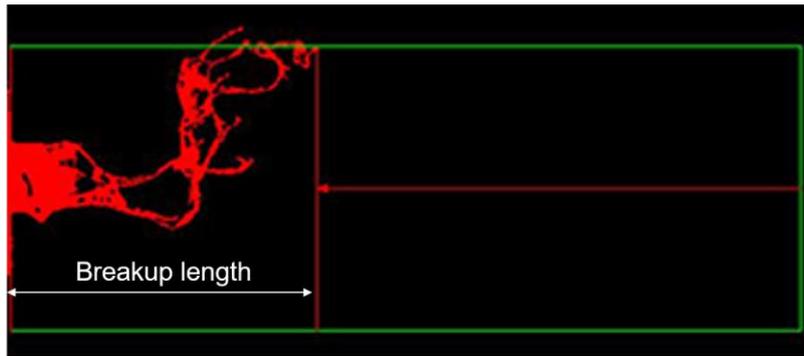**Fig. 4. High viscous liquid breakup in a low-pressure streaming air.**

Fig. 5. Breakup length measurement using image processing.

jet in front of the nozzle. The liquid viscous forces prevent small liquid sub jets to be disintegrated from the liquid jet external surface. The liquid main jet disintegrates similar to the Rayleigh breakup model downstream of the atomizer. However, the head and tail of the disintegrated ligaments produce giant liquid droplets in head and tail due to the intermolecular adhesion forces. The produced droplets appear to have a wide size range including very big droplets and small droplets. The generated small droplets are originating at first from the bag sheet breakup mechanism and later from the Rayleigh breakup mechanism downstream of the atomizer.

The liquid viscosity effect on the breakup length at low and high air pressure at N5 is presented in Fig. 6. The length of the continuous portion of the jet, measured from the nozzle to the longest breakup point where drop formation occurs, is defined as the breakup length (Lefebvre, 1989). The breakup length measurement was challenging, since the instantaneous breakup position is not fix during the atomization process. Therefore, an image processing algorithm has been developed and applied for a minimum of 450 images at various operation conditions. A final step of image processing processes, shown in Fig. 5, indicates the measured breakup length. Error bars represent the standard deviation within the measured time intervals. As it was mentioned before, the viscosity delays the liquid disintegration by identical air and liquid flowrates. The breakup length appears to be longer in higher viscosity operations. As viscosity is increased at $P_a = 0.25$ bar (red bars in Fig. 6), longer ligaments were generated due to high viscosity internal forces. Indeed, the breakup length increased significantly. The breakup length is dependent on liquid viscosity with $L_b \propto \mu_l^{0.30}$ and $L_b \propto \mu_l^{0.46}$ for $P_a = 0.25$ and 0.6 bar, respectively. Apparently, the liquid viscosity dependency increased to some extent with increasing air pressure in the prefilming airblast atomizer.

3.2. PDA Measurements

High-resolution PDA measurements were performed both radially and axially in order to analyze spray properties. Water, four different glycerol-water mixtures, and three different ethanol-water mixtures are employed in the

measurements to investigate the effect of different liquid viscosity and surface tension values on droplet size and droplet velocity downstream the spray. The influence of operation conditions has also been investigated while atomizing liquids with both variable liquid properties.
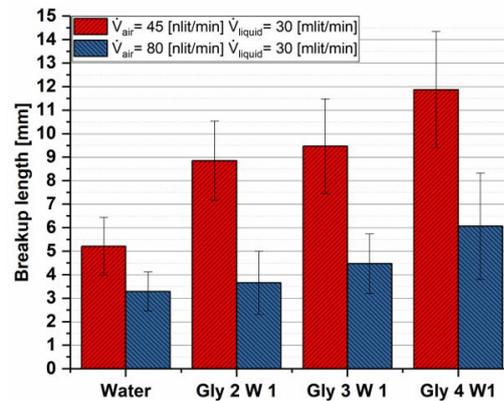

Fig. 6. Influence of the liquid viscosity on the breakup length.

One of the most important mean diameters which is used for applications where it involves the mass transfer, evaporation, and combustion is the Sauter Mean Diameter (SMD) which is used for comparison in the current study. SMD is the diameter of a drop whose ratio of the volume to surface area is the same as that of the entire spray. SMD is given by the Eq. (4)

$$SMD = \frac{\sum N_i D_i^3}{\sum N_i D_i^2} \tag{4}$$

where i denotes the size range considered, N_i the number of drops in the size range i, and D_i the mean diameter of size range i. Other important droplet size representatives, which are used in this study, are $D_{0.1}$ where 10% of the total liquid volume shows smaller droplets, $D_{0.9}$ where 90% of the total liquid volume contains smaller droplets, and $D_{0.5}$ also called mass mean diameter, where 50% of the total liquid volume exhibits smaller droplets. The most commonly used parameter to describe the spray dispersion is the relative span factor, which is determined by the Eq. (5). The relative span factor
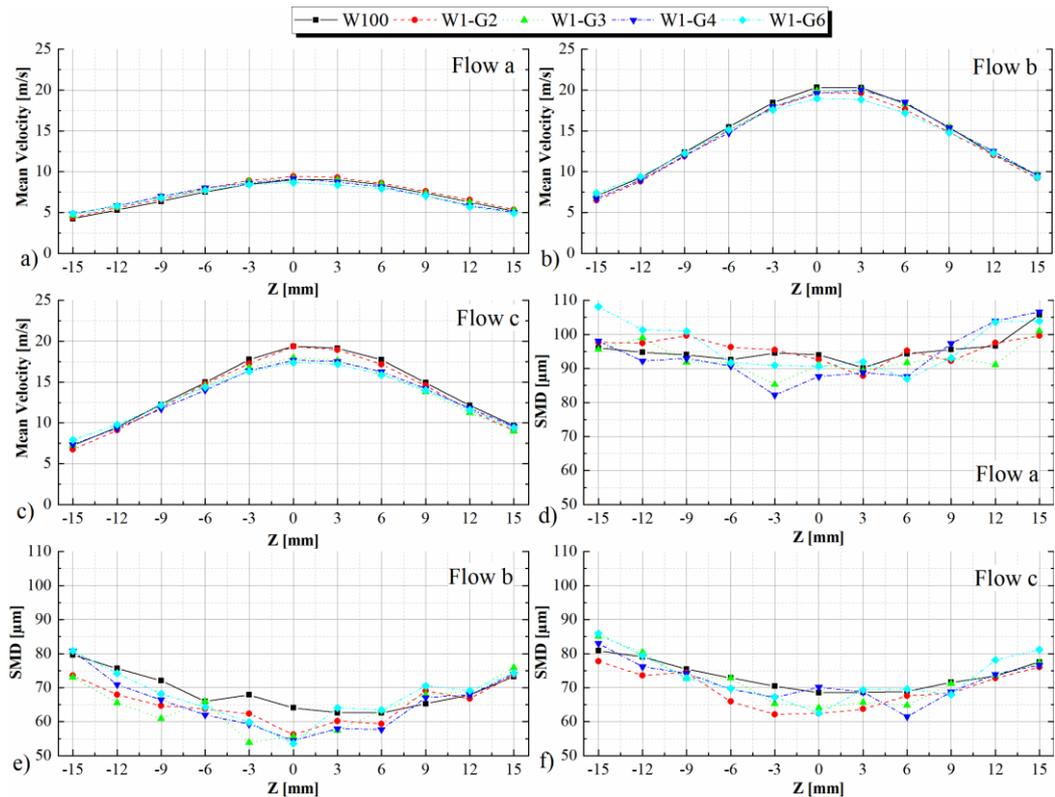
Fig. 7. Influence of the liquid viscosity on the mean velocity (a, b and c) and SMD (d, e, and f) along the radial direction.

gives a direct indication of the range of drop sizes relative to the mass mean diameter (Lefebvre, 1989).

$$\Delta = \frac{D_{0.9} - D_{0.1}}{D_{0.5}} \tag{5}$$

The evaluated operation conditions in the current section are listed in Table 3.

Table 3 Flow conditions in liquid property investigations

	Flow a	Flow b	Flow c
Air Pressure [bar]	0.25	0.6	0.6
Liquid Flowrate [ml/min]	30	30	50

3.2.1. Influence of Viscosity

Radial direction: In Fig. 7, the influence of the liquid viscosity on the mean velocity and Sauter mean diameter along the radial direction using nozzle 5 is shown. As Fig. 7(a), (b), and (c) display a symmetric radial profile of the mean velocity is observed with its maximum on the spray axis. The droplet velocity is slightly reducing in the spray centerline region with increasing the liquid viscosity especially at flow c with a higher liquid flow rate. As it is observed from the previous section, highly viscous liquids take longer to be

disintegrated and they require a higher amount of the energy for the atomization. In consequence, generated droplets are exposed to the annular air flow far away, therefore, their velocity is slightly lower. Furthermore, the influence of the liquid viscosity on the Sauter mean diameter profile in radial direction presents no clear trends (Shown in Fig. 7(d), (e), and (f)). There seems to be a complex tendency between the liquid viscosity and droplet sizes in prefilming airblast atomizers. The liquid flowrate reduces as soon as the liquid viscosity decreases which subsequently increases the relative velocity with air followed by a reduction of droplet sizes. However, it is also known that high viscous liquids delayed the atomization process resulting in larger droplets. But it was observed that the water (1) + glycerol (2) mixture (W1G2) with a lower viscosity produces somewhat smaller droplets at a high liquid flowrate condition (Fig. 7(f)). After comparison of Fig. 7(d) and (e), it was observed that when the air pressure increases, SMD in the entire radial profile for different liquids decreases significantly.

Axial direction: In Fig. 8, the influence of the liquid viscosity on the mean droplet velocity and Sauter mean diameter along the axial direction is presented. As Fig. 8(a), (b), and (c) show, the droplet velocity is slightly higher for higher viscosity liquids in the near field area compared to water (0 to 50 mm). As it was observed in the previous section, ligaments and droplets were generated with different breakup mechanisms at the
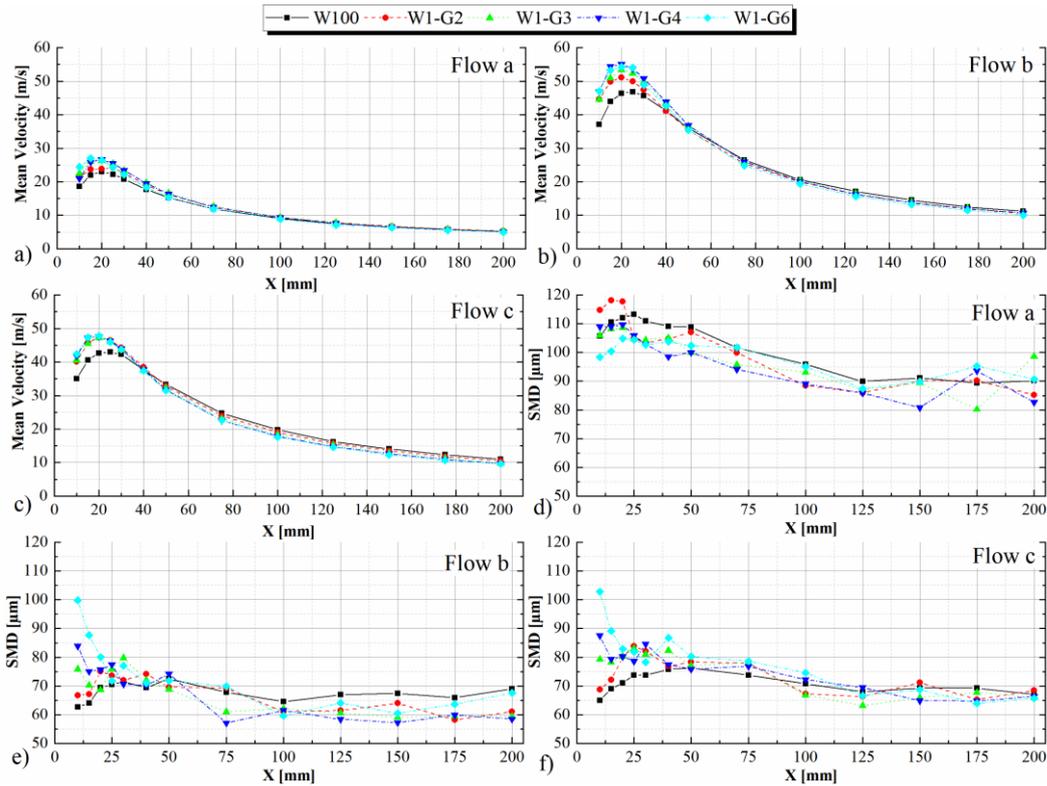
Fig. 8. Influence of the liquid viscosity on the mean velocity (a, b and c) and SMD (d, e, and f) along the axial direction.

vicinity of the nozzle exit by increasing viscosity. Accordingly, very large ligaments and droplets were generated due to higher viscous forces. It seems that, based on the larger inertia of those bigger droplets, they need more time to be accelerated downwards, therefore, they have slightly higher velocity within the near field area. These large droplets with low velocities will be disintegrated further to the smaller droplets during the secondary atomization. It can be observed that droplet velocity differences reduce significantly from about $x = 50$ mm. Consequently, the droplet mean velocity is slightly lower for viscous liquids downstream of the atomizer. The droplet sizes are significantly larger for the liquid with a higher viscosity in the near field region especially in flow b and c with a higher air pressure (shown in Fig. 8(e) and (f)). The large droplets reduce their sizes significantly during the secondary atomization development. Although, the viscosity delays the spray fully-developed region, it is very hard to establish common rules concerning the influence of viscosity on the droplet size downstream of the atomizer (Fig. 8(d), (e), and (f)). The viscosity effect will be dominant with raising the liquid flowrate, accordingly, the droplet size becomes larger with the viscosity increase before the spray development region (Fig. 8(c)). In a low air velocity (Fig. 8(d)), the droplet size increases interestingly with increasing viscosity. The current results suggest that the influence of viscosity depends strongly not only on the spray region but also on air and liquid flowrates.

Droplet size representatives: Fig 9 shows the effect of the viscosity on the evolution of $D_{0.1}$, $D_{0.5}$, $D_{0.9}$ and span along the axial direction at $P_a = 0.6$ bar and $Q = 50$ ml/min. The $D_{0.9}$ shows a fluctuation trend around a nearly constant value for viscous liquids and the water in the identical operating condition plotted in the graph. The $D_{0.9}$ attains its constant value for the viscos liquids, nevertheless, it reduces for water further downstream of the atomizer. Therefore, viscous forces seem to prevent large droplets to go through the long secondary atomization process. The lower vaporization rate for the viscous liquids causes the droplets to attain their size far away from the atomizer. In comparison the $D_{0.1}$ of the viscous liquids decreases initially due to the secondary atomization followed by the constant value after $x = 100$ mm. The size of the $D_{0.1}$ interestingly reduces with increasing of the liquid viscosity at far downstream of the atomizer. This could be due to a lower rate of evaporation in higher viscous liquids because viscos forces make it less likely for molecules on the surface to escape from the liquid and become vapor. $D_{0.5}$ follows a similar trend for the different liquids and it generally increases with increasing the liquid viscosity. As explained earlier, the span of a spray represents the range of droplets in a distribution. As it can be seen at Fig. 9, the span of the spray reveals a different behavior for water compared to the viscos liquids. The span increases significantly with the viscosity along axial direction due to a simultaneous increase of the $D_{0.9}$ difference and a decrease of the $D_{0.1}$ difference.
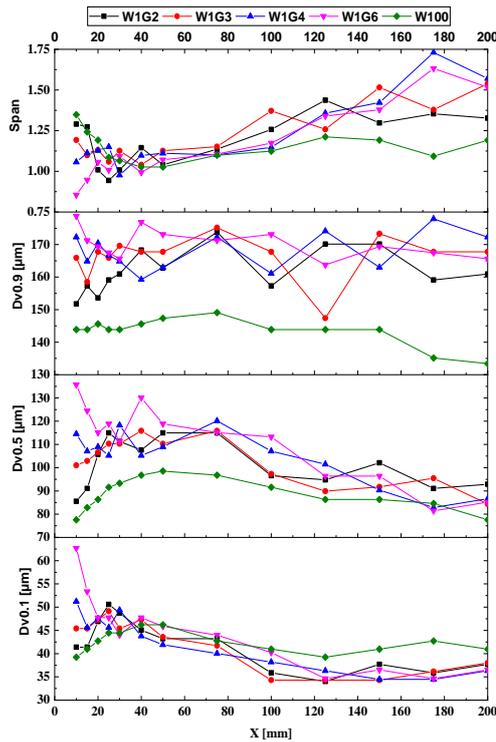
Fig. 9. Influence of the viscosity on D$_{0.1}$, D$_{0.5}$, D$_{0.9}$ and span of the spray (P$_a$= 0.6 bar and Q=50 ml/min).

3.2.2. Influence of Surface Tension

Radial direction: In Fig. 10, the influence of the liquid surface tension on mean velocity and Sauter mean diameter span wise using Nozzle 5 is revealed. Fig 10(a), (b), and (c) show no significant influence of the surface tension on the mean droplet velocity in three different operation conditions. The radial velocity profile of the water+ethanol mixture illustrates a similar trend as water. Although, an increase of the liquid surface tension leads to a considerable reduction on Sauter mean diameter profile in radial direction at all three different flows (see Fig. 10(d), (e), and (f)). A lower surface tension leads to the lower required energy to disintegrate the discharged liquid. Consequently, the liquid surface tension plays an important role in the atomization process of prefilming airblast atomizers.

Axial direction: The influence of the liquid surface tension on mean velocity and Sauter mean diameter along axial direction using Nozzle 5 is presented in Fig 11 (a), (b), and (c) show a small different in the mean droplet velocity of the different liquid up to 50 mm distance in front of the nozzle. The lower surface tension contributes to a lower droplet size influencing the droplets velocities in front of the atomizer. From that region, no significant influence of the surface tension on the mean droplet velocity was observed in all three flows. Similar to the radial profile, the droplets size reduces significantly with a surface tension decrease in the entire 200 mm axial distance on the spray centerline (see Fig. 11(d), (e),

and (f)). Furthermore, as it can be seen the spray fully-developed region appeared closer to the atomizer. Consequently, SMD starts earlier to be increased for the liquid with lower surface tension through all three different operation conditions. It seems that a higher vaporization rate in the low surface tension liquids helps to vaporize significantly the small droplets, as a result, the SMD increase occurred closer to the atomizer according to the liquid's surface tension.

Droplet size representatives: Fig 12 shows the effect of the surface tension on the evolution of $D_{0.1}$, $D_{0.5}$, $D_{0.9}$ and span along the axial direction at $P_a = 0.6$ bar and $Q = 50$ ml/min. The $D_{0.9}$ shows a fluctuation trend around a nearly constant value for low surface tension liquids and the water in the identical operating condition plotted in the graph. The $D_{0.9}$ reduces with higher rate for low surface tension liquids compared with the water further downstream of the atomizer. Therefore, lower surface tension forces seem to facilitate large droplets to go through the droplet surface vaporization. In comparison the size of $D_{0.1}$ decreases considerably with reducing the surface tension along axial direction. The smaller droplets are produced due to lower surface tension forces which play an important role during the disintegration process. $D_{0.1}$ increases gradually for low surface tension liquids far from the atomizer due to the vaporization of very small droplets. $D_{0.5}$ follows a similar trend for the different liquids and it generally decreases with decreasing the liquids surface tension. As it can be seen at Fig. 12, the span of the spray reveals a similar behavior for water compared to the lower surface tension liquids. The span decreases significantly with the surface tension along axial direction due to the simultaneous decrease of the $D_{0.9}$ difference and a large decrease of $D_{0.1}$ and $D_{0.5}$ differences.

Fig. *13* shows the effect of the liquid viscosity and the liquid surface tension on a global SMD. A global SMD (GSMD) is the local volume flux weighted average of local SMD along the radial axis of the spray. Each measurement using each atomizer has a single GSMD for a better comparison and it can be determined by the Eq. (6) at any distance from an atomizer.

$$GSMD_z = \frac{\sum_{z=i}^{z=n} \ddot{V}_i . SMD_i}{\sum_{z=i}^{z=n} \ddot{V}_i} \tag{6}$$

A minor increase of GSMD was observed with liquid viscosity variations from 22 to 111 mPas (shown at Fig. 13(a)). The liquid viscosity dependencies, which empirically correlated with a power law, are $\mu^{0.01}$, $\mu^{0.02}$, and $\mu^{0.03}$ for flow a, flow b, and flow c, accordingly. However, the liquid surface tension dependencies are $\sigma^{0.29}$, $\sigma^{0.70}$, and $\sigma^{0.54}$ for flow a, flow b, and flow c, respectively, which shows a significant effect. It appeared that surface tension sensitivities on GSMD become higher with increasing the air pressure from 0.25 bar to 0.6 bar in prefilming coaxial airblast atomizers.
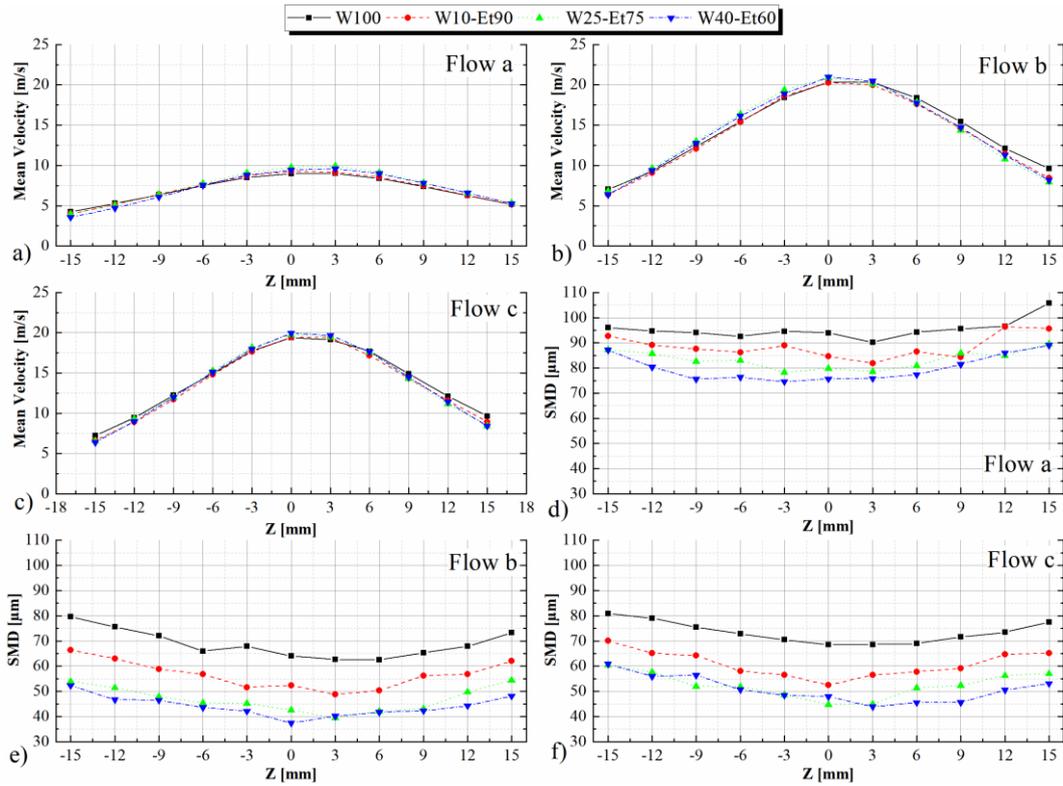
Fig. 10. Influence of the liquid surface tension on mean velocity (a, b and c) and SMD (d, e, and f) along radial direction.
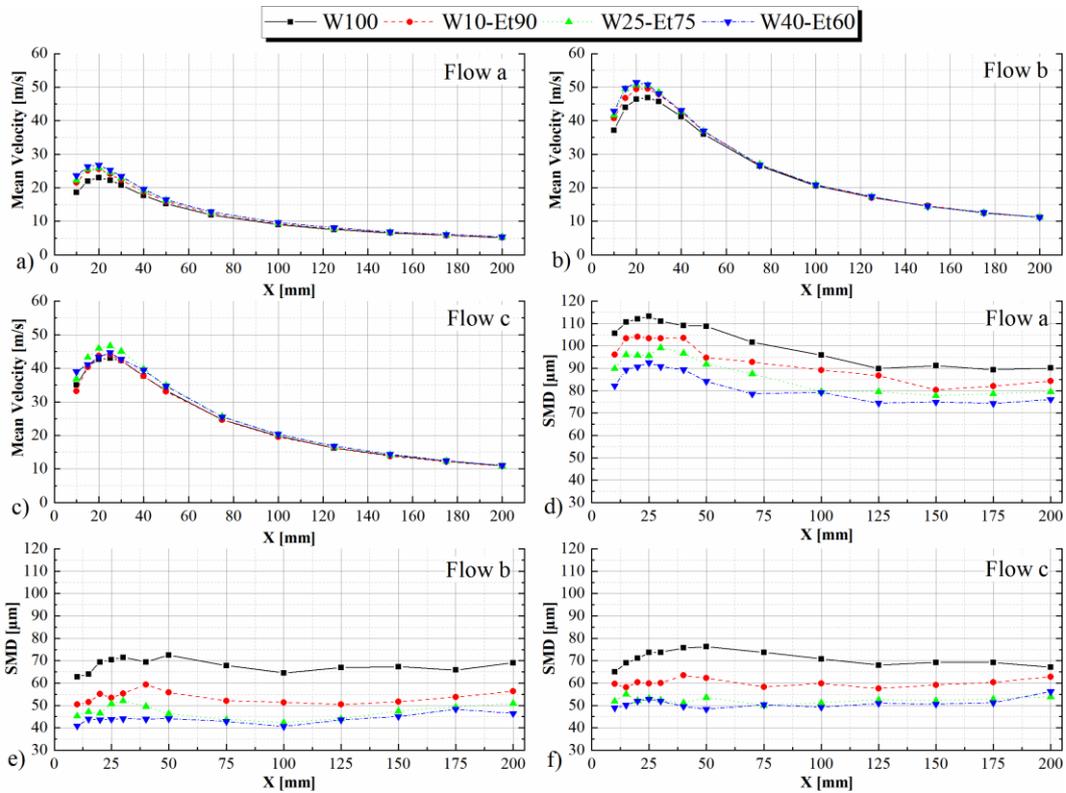

Fig. 11. Influence of the liquid surface tension on mean velocity (a, b and c) and SMD (d, e, and f) along axial direction.
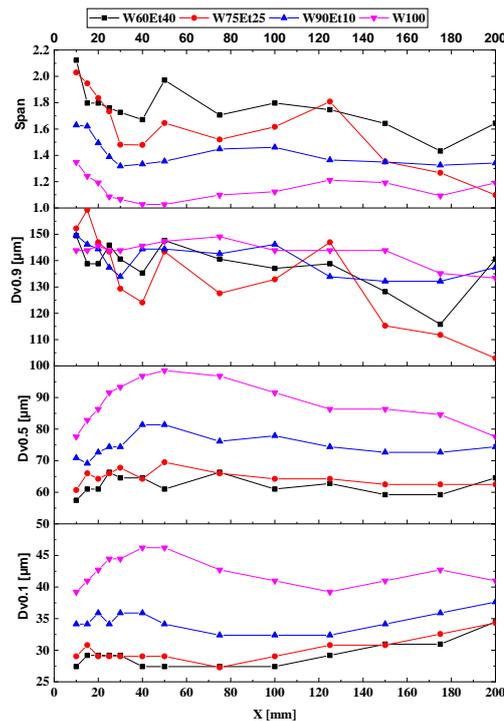
Fig. 12. Influence of the surface tension on $D_{0.1}$, $D_{0.5}$, $D_{0.9}$ and span of the spray (P_a = 0.6 bar and Q =50 ml/min).
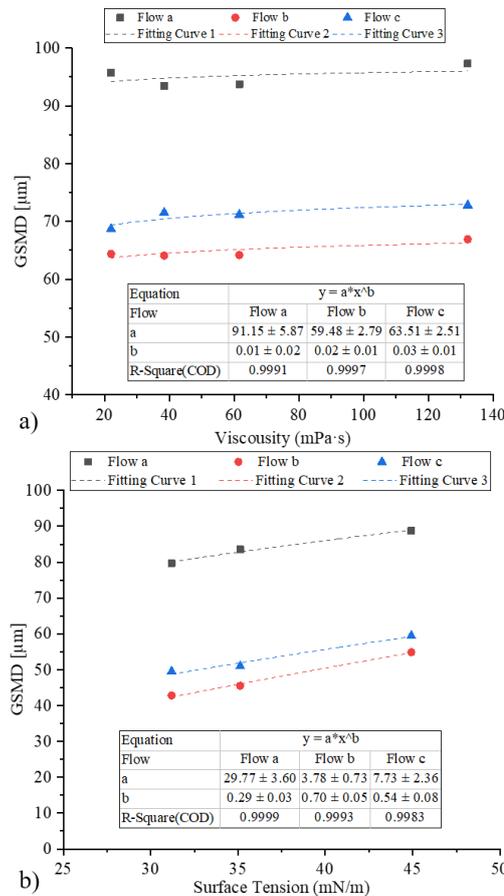

Fig. 13. The effect of (a) viscosity and (b) surface tension on GSMD at three different operation conditions (Table 3).

3.3. Dimensional Analysis

In order to develop a unique functional relationship from experimentally measured droplet sizes in different operation conditions, a dimensional analysis has been performed. This method uses a set of dimensionless ratios to reduce the number of variables which are characterizing a physical application. In the first step, the relevant parameters given by the experiment which influence the atomization of the liquid in different atomizers are required to be identified. In the current study, SMD was noticed to be a function of the below given relevant process parameters:

$$SMD = f(d_e, d_i, \sigma, \mu_l, \rho_a, \rho_l, U_a, U_l) \tag{7}$$

The important process parameters identified in the Eq. (8) were transformed into dimensionless numbers by using the π-theorem (Buckingham, 1914). As a result, a reduced set of relevant dimensionless numbers was obtained in the Eq. (8) leading to the following model,

$$\frac{GSMD}{d_e} = C(Re_l)^{c_1}(We_{rel})^{c_2} \tag{8}$$

The coefficients of the proposed dimensionless process model are determined separately by a power law using the Origin 2018 software. A least-square fit has been employed to correlate the determined model with the measurement results which was used also by previous researchers (Glathe, Wozniak, & Richter, 2001; Petit *et al.*, 2015). Identified coefficients on the basis of the experimental results were listed in Table 4. Additionally, the coefficient of determination (COD) R^2 representing the model accuracy of each non-dimensional parameters is presented. C is an empirical constant and will be determined for each air pressure range accordingly.

The derived exponents C_1 and C_2 of Eq. (8) which are shown in Table 4 describe the influence of main characteristics of the spray. The liquid Reynolds number has a direct positive influence on droplet size the influence of which increases slightly from 0.10 to 0.18 with increasing air pressure from 0.5 bar to 1.5 bar. The Reynolds number effect is also more pronounced at higher air pressure. The relative Weber number is the most important parameter on the liquid atomization, as air momentum provides the required energy initiating the disintegration of the liquid jet. The negative direct influence of the relative Weber number increases from -0.39 to -0.65 with increasing air pressure.

Fig. 14 shows the adjustment between the proposed model and experimental measurement data in four different air pressure groups. The satisfying correlation quality between the measurement data and the fitted functions is expressed by the coefficient of multiple determination (r-square) and the residual sum of squares shown in Fig. 14(a) to Fig. 14(d). The nozzle geometry effect (d_e & d_l) and the liquid properties are considered in the proposed model. The shades around the fitted curve present the

Table 4 Model coefficients of Eq. (8) for predicting SMD in prefilming airblast atomizers

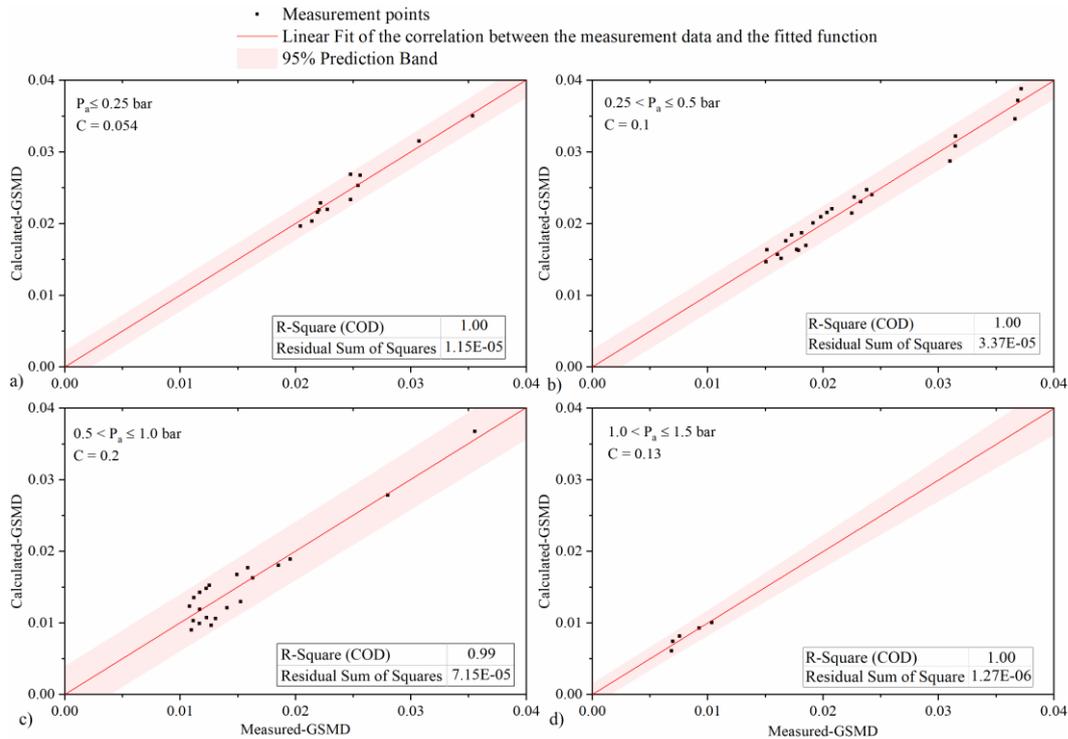| Model coefficient	Variables	Value		R^2 (COD)
c_1	Re_l	$P_a = 0.5\ bar$	**0.10**	0.99
		$P_a = 0.75\ bar$	**0.13**	0.98
		$P_a = 1\ bar$	**0.16**	0.94
		$P_a = 1.5\ bar$	**0.18**	0.86
c_2	We_{rel}	$P_a \leq 0.25\ bar$	**-0.22**	0.99
		$0.25 < P_a \leq 0.5\ bar$	**-0.39**	0.95
		$0.5 < P_a \leq 1.0\ bar$	**-0.58**	0.87
		$1.0 < P_a \leq 1.5\ bar$	**-0.65**	0.98

Fig. 14. Predicted versus experimental dimensional droplet diameters for the prefilming airblast atomizers at different air pressure ranges. a) $P_a \leq 0.25$ bar, b) $0.25 < P_a \leq 0.5$ bar, c) $0.5 < P_a \leq 1.0$ bar and d) $1.0 < P_a \leq 1.5$ bar.

prediction band for the 0.95 confidence level. The prediction band is the interval within which 95% of all the experimental values in a series of repeated measurements are expected to fall. Indeed, there is 95% confidence to say that an expected data point will fall within this interval. The empirical constant (C) is extracted and it is shown for each plot.

4. SUMMERY AND CONCLUSIONS

In this study, the process of the development of prefilming airblast atomizers has been experimentally described. One of the main goals of this work is to understand the liquid film breakup mechanism near the nozzle exit using high speed shadowgraphy and to investigate the effect of liquid properties on the physics of the liquid sheet breakup. Important features like the breakup length of the liquid sheet has been quantified varying the liquid viscosity. The breakup length appears to be longer in higher viscosity operations due to high viscosity internal forces. Apparently, the liquid

viscosity dependency increased with used higher air pressure in the prefilming airblast atomizer.

A minor increase of the GSMD was observed with liquid viscosity variations from 22 to 111 mPas, however, the liquid surface tension was verified to play an important role in the atomization process at prefilming airblast atomizers. The current results suggest that the influence of both investigated liquid properties on GSMD depends strongly not only on different spray regions but also on air and liquid flowrates.

According to the available experimental data, it has been possible to develop an original and descriptive model based on a dimensional approach at different air pressure ranges. A unique equation was proposed considering the effects of the geometry of the atomizing systems through a unique equation. The influence of two main nondimensional numbers showed different sensitivities depending on the pressure range and was quantified by fitting the data to appropriate correlation functions. In conclusion, the specific regime determination according to the

application operational conditions enhance significantly the atomizer design process.

REFERENCES

Babinsky, E. and P. E. Sojka (2002). Modeling drop size distributions. *Progress in Energy and Combustion Science* 28(4), 303-329.

Buckingham, E. (1914). On Physically Similar Systems; Illustrations of the Use of Dimensional Equations. *Physical Review* 4(4), 345-376.

Chaussonnet, G., Laroche, T., Lieber, C., Holz, S., Koch, R., & Bauer, H. (2018). Investigation of the liquid accumulation characteristics in planar prefilming airblast atomization. In *14th Triennial International Conference on Liquid Atomization and Spray System*. Chicago, IL, USA.

Gepperth, S., R. Koch and H. J. Bauer (2013). Analysis and comparison of primary droplet characteristics in the near field of a prefilming airblast atomizer. In *ASME Turbo Expo 2013: Turbine Technical Conference and Exposition* (p. V01AT04A002-V01AT04A002). American Society of Mechanical Engineers.

Gepperth, S., A. Müller, R. Koch and H. J. Bauer (2012). Ligament and Droplet Characteristics in Prefilming Airblast *Atomization* 320(1975), 2012.

Glathe, A., G. Wozniak and T. Richter (2001). The influence of eccentricity on the performance of a coaxial prefilming air-assist atomizer. *Atomization and Sprays* 11(1), 21-33.

Guildenbecher, D. R., C. López-Rivera and P. E. Sojka (2009). Secondary atomization. *Experiments in Fluids* 46(3), 371-402.

Hardalupas, Y. and J. H. Whitelaw (1994). The characteristics of sprays produced by coaxial airblast atomisers. *Journal of Propulsion and Power* 10(4), 453-460.

Lefebvre, A. H. (1989). *Atomization and Sprays. Corp., New York*. Taylor & Francis.

Lefebvre, A. H. and V. G. McDonell (2017). *Atomization and Sprays, Second Edition*. CRC Press.

Liu, H. F., X. Gong, W. F. Li, F. C.Wang and Z. H. Yu (2006). Prediction of droplet size distribution in sprays of prefilming air-blast atomizers. *Chemical Engineering Science* 61(6), 1741-1747.

Lorenzetto, G. E., and A. H. Lefebvre (1977). Measurements of Drop Size on a Plain-Jet Airblast Atomizer. *AIAA Journal* 15(7), 1006-1010.

Petit, J., S. Mejean, P. Accart, L. Galet, P. Schuck, C. Le Floch-Fouere, G. Delaplace and R. Jeantet (2015). A dimensional analysis approach for modelling the size of droplets formed by bi-fluid atomisation. *Journal of Food Engineering*, 149, 237-247.

Rizk, N. K. and A. H. Lefebvre (1984). Spray characteristics of plain-jet airblast atomizers. *Journal of Engineering for Gas Turbines and Power* 106(3), 634–638.

Rizkalla, A. A. and A. H. Lefebvre (1975). Influence of Air and Liquid Properties on Airblast Atomizer. *Journal of Engineering for Power* 97(2), 173-177.

Roudini, M. and G. Wozniak (2018). Experimental Investigation of Spray Characteristics of Pre-filming Air-blast Atomizers. *Journal of Applied Fluid Mechanics* 11(6), 1455-1469.

Sellens, R. W. and T. A. Brzustowski (1985). A prediction of the drop size distribution in a spray from first principles. *Atomisation Spray Technology* 1, 89-102.

Urbán, A., M. Zaremba, M. Malý, V. Józsa and J. Jedelský (2017). Droplet dynamics and size characterization of high-velocity airblast atomization. *International Journal of Multiphase Flow* 95, 1-11.

Zhou, W. X., and Z. H. Yu (2000). Multifractality of drop breakup in the air-blast nozzle atomization process. *Physical Review E*, 63(1), 16302.